JOURNAL OF INTEGRAL EQUATIONS
AND APPLICATIONS
Volume 21, Number 2, Summer 2009

THE DIRECT METHOD OF FUNDAMENTAL SOLUTIONS AND THE INVERSE KIRSCH-KRESS METHOD FOR THE RECONSTRUCTION OF ELASTIC INCLUSIONS OR CAVITIES

CARLOS J. S. ALVES AND NUNO F. M. MARTINS

Communicated by Charles Groetsch

This paper is dedicated to Professor Rainer Kress on the occasion of his 65th birthday.

ABSTRACT. In this work we consider the inverse problem of detecting inclusions or cavities in an elastic body, using a single boundary measurement on an external boundary. We discuss the identifiability questions on shape reconstruction, presenting counterexamples for Robin boundary conditions or with additional unknown Lamé parameters. Using the method of fundamental solutions (MFS) we adapt a method introduced twenty years ago by Andreas Kirsch and Rainer Kress [**20**] (in the context of an exterior problem in acoustic scattering) to this inverse problem in a bounded domain. We prove density results that justify the reconstruction of the solution from the Cauchy data using the MFS. We also establish some connections between this linear part of the Kirsch-Kress method and the direct MFS, through matrices of boundary layer integrals. Several numerical examples are presented, showing that with noisy data we were able to retrieve a fairly good reconstruction of the shape (or of its convex hull) with this MFS version of the Kirsch-Kress method.

1. Introduction.

The identification of inclusions or cavities in an elastic body from external boundary measurements is a problem in nondestructive testing. This is an inverse problem that aims to reconstruct the shape and location of the burried object from the knowledge of the Cauchy data. This problem has been addressed in the literature for both scalar and vectorial potential problems with different boundary conditions. For the Laplace equation, with applications in

Received by the editors on April 27, 2007, and in revised form on May 28, 2008.
DOI:10.1216/JIE-2009-21-2-153

thermal imaging see for instance [**9, 15, 16**] and more recently [**10**] where an unknown Robin boundary condition was considered. For the elasticity (or elastodynamic) system, see the review paper by M. Bonnet [**8**]. Some recent works considered the detection of small diameter inclusions (eg. [**2, 4**]) or spherical inclusions (eg. [**6**]). The detection of elastic cavities and inclusions can also be analysed in a different framework in terms of a change in the elastic material properties (e.g. [**1, 26, 27**]).

In this work, we address the aforementioned inverse problem considering a single boundary measurement on an accessible part of the external boundary. The buried object is either a rigid inclusion (defined by a Dirichlet boundary condition), a cavity (defined by a Neumann like boundary condition) or a more general inclusion (defined by a Robin like boundary condition). The identifiability questions are discussed in Section 2 and in Section 3 we focus on the numerical resolution of the inverse problem. We propose a numerical scheme that connects the Method of Fundamental Solutions (MFS), proposed forty years ago by Kupradze and Aleksidze [**22**], and the Kirsch-Kress Method (KKM), proposed twenty years ago [**20**]. The MFS was usually presented as a numerical method for direct problems, but it has gained recently some popularity as a method to solve some Cauchy problems (eg. [**23**]). This feature was already present in the original formulation of the Kirsch-Kress Method (for acoustic scattering) using single layer potentials, that consists in two parts: (i) linear part - resolution of the Cauchy problem, (ii) nonlinear part - recovering the level set by an optimization technique. This connection is here made clear by analysing the operator matrices with boundary potentials for both the MFS and the KKM. Although density results are deduced for both methods, these share an ill-conditioned feature that can be dealt with a Tikhonov regularization technique.

In Section 4 several numerical examples show the possibilities (and some difficulties) of the MFS used in the KKM sense, for these elastic inverse problems, considering unknown rigid inclusions. This technique was previously tested for scalar (Laplace) problems with better reconstruction results[1], which can be explained by the difficulties in obtaining a level curve in the vectorial case. Nevertheless this proved to be a

[1]Communication by the authors in the International Workshop on Integral Equations and Shape Reconstruction (Göttingen, Germany, 2007).

quite fast numerical scheme that enables a good approximation of the location and shape of the unknown inclusion even with considerable noisy data.

2. Direct and Inverse Problem. We consider an isotropic and homogeneous elastic body $\Omega \subset \mathbb{R}^d$ $(d = 2, 3)$ with inclusions or cavities represented by ω. We assume that Ω, ω are open, bounded and simply connected sets with regular (C^1) boundaries $\Gamma = \partial\Omega$ and $\gamma = \partial\omega$ such that $\overline{\omega} \subset \Omega$. We define the domain of elastic propagation by

$$\Omega_c := \Omega \setminus \overline{\omega}.$$

Note that $\partial\Omega_c = \Gamma \cup \gamma$.

In linearized elasticity, using Hooke's law, the stress tensor σ is defined in terms of the displacement vector $\mathbf{u}$ by

$$\sigma_{\lambda,\mu}(\mathbf{u}) = \lambda(\nabla \cdot \mathbf{u})\mathbf{I} + \mu\left(\nabla\mathbf{u} + \nabla\mathbf{u}^\top\right)$$

where λ and μ are the *Lamé coefficients.* When there is no body force and the body is in static equilibrium, the equations of motion resume to a null divergence of the stress, giving the Lamé system of equations

$$\nabla \cdot \sigma_{\lambda,\mu}(\mathbf{u}) = \mathbf{0}.$$

We will write $\Delta^*_{\lambda,\mu}\mathbf{u} := \nabla \cdot (\sigma_{\lambda,\mu}(\mathbf{u}))$, noticing that

$$\nabla \cdot \sigma_{\lambda,\mu}(\mathbf{u}) = \mu\Delta\mathbf{u} + (\lambda + \mu)\nabla\nabla \cdot \mathbf{u},$$

and we will use the notation $\partial^*_{\lambda,\mu}\mathbf{u} := \sigma_{\lambda,\mu}(\mathbf{u})\mathbf{n}$ for the surface traction vector, where $\mathbf{n}$ is the outward normal vector.

Direct problem. Given $\mathbf{g} \in H^{1/2}(\Gamma)^d$, determine $\partial^*_{\lambda,\mu}\mathbf{u}$ on Γ, such that $\mathbf{u}$ satisfies

$$\begin{cases} \Delta^*_{\lambda,\mu}\mathbf{u} = \mathbf{0} & \text{in } \Omega_c \\ \mathbf{u} = \mathbf{g} & \text{on } \partial\Omega = \Gamma \\ \mathcal{B}_\gamma\mathbf{u} = \mathbf{0} & \text{on } \partial\omega = \gamma \end{cases} \tag{1}$$

with known Lamé coefficients $\lambda, \mu > 0$. The boundary operator $\mathcal{B}_\gamma$ is defined by

$$\mathcal{B}_\gamma\mathbf{u} = a\partial^*_{\lambda,\mu}\mathbf{u} + \mathbf{Z}_a\mathbf{u} \tag{2}$$

where $a \in \{0,1\}$ is constant and $\mathbf{Z}_a$ is a $\mathrm{L}^\infty(\gamma)$ positive semidefinite matrix function such that $\mathbf{Z}_0 = \mathbf{I}$.

• If $a = 0$ then $\mathcal{B}_\gamma$ is the Dirichlet operator. In this case, ω is a rigid inclusion and (1) will be denoted by $(\mathcal{P}_D)$.

• When $\mathbf{Z}_1 = \mathbf{0}$, $\mathcal{B}_\gamma$ is the Neumann operator (ω is a cavity) and (1) will be denoted by $(\mathcal{P}_N)$.

• More generally, we consider $\mathcal{B}_\gamma$ as the Robin operator ($\mathbf{Z}_1 \neq \mathbf{0}$). We denote this problem by $(\mathcal{P}_R)$.

It is well known that $(\mathcal{P}_D)$, $(\mathcal{P}_N)$ and $(\mathcal{P}_R)$ are well posed with solution $\mathbf{u} \in H^1(\Omega_c)^d$.

Inverse problem. From a single pair of displacement and surface traction data $(\mathbf{g}, \partial^*_{\lambda,\mu}\mathbf{u})$ on a part Σ of the external boundary, ie. $\Sigma \subseteq \Gamma = \partial\Omega$, we aim to identify the shape of the internal boundary $\gamma = \partial\omega$ and the boundary condition on γ.

It is well known that the recovery of a solution from Cauchy data is an ill posed problem in the Hadamard sense. In terms of the inverse problem, this means (assuming uniqueness of the inverse problem) noise sensitive reconstructions. The uniqueness of the inverse problem is addressed in the next section.

2.1. *Identifiability.*

2.1.1. *Non-identifiability cases (single measurement)*

(i) *Robin boundary condition.* As shown by Cakoni and Kress in [**10**], for the Laplace equation, a single boundary measurement may not suffice to identify an inclusion ω with Robin boundary conditions. This non identification also occurs in the elastic case. For instance, consider the function defined in $\mathbb{R}^2 \setminus \{\mathbf{0}\}$ by

$$\mathbf{u}(\mathbf{x}) = \mathbf{x} - \nabla \log|\mathbf{x}| \tag{3}$$

and the annular domain $\Omega_c = \Omega \setminus \overline{\omega}$, where

$$\Omega = B(\mathbf{0}, P) = \left\{\mathbf{x} \in \mathbb{R}^2 : |\mathbf{x}| < \mathrm{P}\right\}, \omega = B(\mathbf{0}, \rho)$$

and $0 < \rho < \mathrm{P}$. A forward computation gives, on $\gamma = \partial\omega$

$$\partial^*_{\lambda,\mu}\mathbf{u}\Big|_\gamma = \frac{2+4\rho^2}{\rho^2}\mathbf{n} \ \wedge \ \mathbf{u}\Big|_\gamma = -\frac{1-\rho^2}{\rho}\mathbf{n}.$$

Since $\mathbf{u}$ solves the Lamé system in $\mathbb{R}^2 \setminus \{\mathbf{0}\}$, we have

$$\begin{cases} \Delta^*_{\lambda,\mu}\mathbf{u} = 0 & \text{in } \Omega_c \\ \mathbf{u} = \mathbf{g} & \text{on } \Gamma \\ \partial^*_{\lambda,\mu}\mathbf{u} + \mathbf{Z}_\rho\mathbf{u} = \mathbf{0} & \text{on } \gamma \end{cases}$$

where $\mathbf{g}$ is the restriction of $\mathbf{u}$ to $\Gamma = \partial\Omega$ and

$$\mathbf{Z}_\rho = \frac{2+4\rho^2}{\rho(1-\rho^2)}\mathbf{I}.$$

Since the function $\rho \to \frac{2+4\rho^2}{\rho(1-\rho^2)}$ is not injective for $0 < \rho < 1$ (... it has a derivative zero in $\rho = \frac{1}{2}\sqrt{-5+\sqrt{33}} \approx 0.43$) then at least two circular inclusions generate the same Cauchy data on Γ.

(ii) *Unknown Lamé coefficients.* In [**27**], Nakamura and Uhlmann obtained, in a more general framework, a sufficient condition for the identification of Lamé coefficients, assuming the knowledge of the Dirichlet to Neumann map. A further analysis of the previous example shows that one measurement may not suffice for the identification of these constants. For instance, if $\rho = 1 < \mathrm{P}$, then $\mathbf{u}$ defined in (3) is the solution of the Dirichlet problem

$$\begin{cases} \Delta^*_{\lambda_0,\mu_0}\mathbf{u} = 0 & \text{in } \Omega_c \\ \mathbf{u} = \mathbf{g} & \text{on } \Gamma \\ \mathbf{u} = \mathbf{0} & \text{on } \gamma \end{cases}$$

with unknown Lamé constants λ_0 and μ_0. The Neumann data on Γ is

$$\partial^*_{\lambda_0,\mu_0}\mathbf{u}|_\Gamma = \frac{2(\mu_0 + \mathrm{P}^2(\lambda_0+\mu_0))}{\mathrm{P}^2}\mathbf{n}$$

therefore, the (non empty) set of Lamé constants

$$\left\{(\lambda,\mu) \in \mathbb{R}^2_+ : \mu - \mu_0 = \frac{\mathrm{P}^2}{1+\mathrm{P}^2}(\lambda_0 - \lambda)\right\}$$

generates the same data on the boundary, and identification is not possible.

2.1.2. *Identifiability results.* We start with a proof that extends to the elastic case the Holmgren lemma and analytic continuation arguments.

Lemma 1. *Let $\Omega \subset \mathbb{R}^d$ with C^1 boundary $\Gamma = \partial\Omega$ and consider $\Sigma \subset \Gamma$ open in the topology of Γ. If $\mathbf{f} \in \mathcal{E}'(\Omega)$, a compactly supported distribution, with support $\overline{\Omega}_{\mathbf{f}} \subset \Omega$ and $\Delta^*_{\lambda,\mu}\mathbf{u} = \mathbf{f}$ in Ω with null Cauchy data on Σ then $\mathbf{u} = \mathbf{0}$ in Ω_Σ, where Ω_Σ is the connected component of $\Omega \setminus \overline{\Omega}_{\mathbf{f}}$ such that $\Sigma \subset \partial\Omega_\Sigma$.*

Proof. Consider the extension $\widetilde{\mathbf{u}}$ of $\mathbf{u}$ to the whole space by taking $\widetilde{\mathbf{u}} = 0$ in $\mathbb{R}^d \setminus \overline{\Omega}$. This extension can be given in convolution form by the boundary layers (e.g. [**30**] for the notation)

$$\widetilde{\mathbf{u}} = \Phi * \mathbf{f} - \Phi * [\partial^*_{\lambda,\mu}\mathbf{u}]\delta_\Gamma + \partial^*_{\lambda,\mu}(\Phi * [\mathbf{u}]\delta_\Gamma) \tag{4}$$

where δ_Γ denotes the surface delta-characteristic distribution and $[\cdot]$ denotes the boundary jump. By hypothesis, both interior and exterior traces on Σ are null and $[\partial^*_{\lambda,\mu}\mathbf{u}]|_\Sigma = [\mathbf{u}]|_\Sigma = \mathbf{0}$, therefore

$$\widetilde{\mathbf{u}} = \Phi * \mathbf{f} - \Phi * [\partial^*_{\lambda,\mu}\mathbf{u}]\delta_{\Gamma\setminus\Sigma} + \partial^*_{\lambda,\mu}(\Phi * [\mathbf{u}]\delta_{\Gamma\setminus\Sigma}).$$

Since the fundamental solution Φ is analytic in $\mathbb{R}^d \setminus \{\mathbf{0}\}$ then this representation implies that $\widetilde{\mathbf{u}}$ is analytic in $\mathbb{R}^d \setminus (\overline{\Omega}_{\mathbf{f}} \cup (\Gamma \setminus \Sigma))$. On the other hand, $\widetilde{\mathbf{u}} = \mathbf{0}$ in $\mathbb{R}^d \setminus \overline{\Omega}$ hence, by analytic continuation through Σ, the solution $\mathbf{u}$ is null in those connected components. □

Remark 2. The previous Lemma includes the case of distributions $\mathbf{f}$ that arise from the representation of boundary problems on the cavities ω, in terms of $\mathbf{f} = \alpha\delta_\gamma + \partial^*_{\lambda,\mu}(\beta\delta_\gamma)$. This proof can be extended to other linear elliptic differential operators with constant coefficients, where the fundamental solution exists (Malgrange-Ehrenpreis theorem) and is analytic in $\mathbb{R}^d \setminus \{\mathbf{0}\}$, using the integral representation formulation.

We now address the identification of inclusions or cavities defined by homogeneous Dirichlet or Neumann conditions. Denote by $\mathcal{R}_\Omega$ the linear space of rigid displacements, $\mathcal{R}$, in Ω. In 2D,

$$\mathcal{R} = \mathrm{span}\{(1,0),(0,1),(-x_2,x_1)\}$$

and in 3D

$$\mathcal{R} = \mathrm{span}\{(1,0,0),(0,1,0),(0,0,1),(-x_2,x_1,0),(0,-x_3,x_2),(x_3,0,-x_1)\}.$$

Theorem 3. *Let $\Sigma \subset \Gamma$ be an open set in the topology of Γ and $\mathbf{g} \in H^{1/2}(\Gamma)^d$ such that the restriction $\mathbf{g}|_\Sigma \notin \mathcal{R}_\Sigma$. Then, the Cauchy data $(\mathbf{g}, \partial^*_{\lambda,\mu}\mathbf{u})$ on Σ, where $\mathbf{u}$ solves $(\mathcal{P}_D)$ or $(\mathcal{P}_N)$, determines uniquely ω and the boundary condition on γ.*

Proof. We start by proving that ω is fully identified from Cauchy data on Σ. Suppose that Ω_c^1 and Ω_c^2 are different non-disjoint propagation domains with boundaries

$$\partial\Omega_c^1 = \Gamma \cup \gamma_1, \qquad \partial\Omega_c^2 = \Gamma \cup \gamma_2,$$

where γ_j refer to the boundary of the inclusion/cavity ω_j.

Denote by $\mathbf{u}_i$ the solution of problem $(\mathcal{P}_D)$ or $(\mathcal{P}_N)$ in the domain Ω_c^i. We show that, if

$$\mathbf{u}_1|_\Sigma = \mathbf{u}_2|_\Sigma, \qquad \partial^*_{\lambda,\mu}\mathbf{u}_1|_\Sigma = \partial^*_{\lambda,\mu}\mathbf{u}_2|_\Sigma$$

then $\mathbf{u}_1 \in \mathcal{R}_{\overline{\Omega_c^\#}}$, where $\Omega_c^\#$ denotes the connected component of $\Omega_c^1 \cap \Omega_c^2$ that contains Γ.

By the previous Lemma, the same Cauchy data on Σ implies

$$\mathbf{u}_1 = \mathbf{u}_2 \qquad \text{in } \Omega_c^\#.$$

Now, $\partial\Omega_c^\# = \Gamma \cup \gamma_1^\# \cup \gamma_2^\#$ with $\gamma_j^\# \subset \gamma_j$ and $\gamma_1^\# \cap \gamma_2^\# = \varnothing$. Without loss of generality assume that $\gamma_2^\#$ is not empty. If $\Omega_c^1 \neq \Omega_c^2$ then we can distinguish two cases:

Case 1: $\Omega_c^1 \cap \Omega_c^2$ is connected, ie. $\Omega_c^1 \cap \Omega_c^2 = \Omega_c^\#$. Consider $\sigma = \omega_2 \setminus \overline{\omega}_1 \subset \Omega_c^1$ which is an open set with boundary $\partial\sigma \subset \gamma_2^\# \cup \gamma_1$. It is clear that $\Delta^*_{\lambda,\mu}\mathbf{u}_1 = 0$ in σ and on γ_1 we have null Dirichlet/Neumann data. By the previous Lemma, $\mathbf{u}_1$ has also null Dirichlet/Neumann data on $\gamma_2^\#$.

Case 2: $\Omega_c^1 \cap \Omega_c^2$ is not connected. In this case, take σ as the connected component of $\Omega_c^1 \setminus \overline{\Omega_c^\#}$ that intersects ω_2. Again, $\partial\sigma \subset \gamma_2^\# \cup \gamma_1$.

In both cases we have

$$\text{(5)} \qquad \begin{cases} \Delta^*_{\lambda,\mu}\mathbf{u}_1 = 0 & \text{in } \sigma \\ \mathbf{u}_1 = 0 & \text{in } \partial\sigma_D \\ \partial^*_{\lambda,\mu}\mathbf{u}_1 = 0 & \text{in } \partial\sigma_N \end{cases}$$

where $\partial\sigma_D, \partial\sigma_N \subset \partial\sigma$ are open and $\partial\sigma = \overline{\partial\sigma_D} \cup \overline{\partial\sigma_N}$. Thus, $\mathbf{u_1}$ is null on σ (a rigid displacement, if (5) is a pure Neumann problem) and we conclude, by analytic continuation, that $\mathbf{u_1} \in \mathcal{R}_{\overline{\Omega_c^\#}}$. Since $\Sigma \subset \overline{\Omega_c^\#}$ and $\mathbf{g}|_\Sigma = \mathbf{u}_1|_\Sigma$ then $\mathbf{g}|_\Sigma \in \mathcal{R}_\Sigma$, which contradicts the hypothesis. The conclusion $\Omega_c^1 = \Omega_c^2$ (and therefore $\omega_1 = \omega_2$) follows.

For the second part of the proposition, we note that since $\Omega_c^1 = \Omega_c^2$ then, by the previous Lemma, a solution of $\Delta^*_{\lambda,\mu}\mathbf{u} = 0$ in Ω_c^1 with null Cauchy data on $\gamma \subset \partial\Omega_c^1$ must vanish in Ω_c^1. Thus, $\mathbf{g}|_\Sigma = \mathbf{0} \in \mathcal{R}_\Sigma$ which contradicts the hypothesis. Therefore, the boundary condition on γ is fully identified by the data on Σ. □

Remark 4.

1. As shown in the non-identifiability counter-examples, the previous result can not be extended to the Robin problem. In the interior boundary problem (5) the boundary condition could be defined by piecewise Robin coefficients $\mathbf{Z}_j$ (positive definite matrices) but the normal direction in $\partial^*_{\lambda,\mu}$ would have opposite sign on $\partial\sigma$.

2. If ω is a disjoint union of simply connected sets then the result is still valid if on the boundary of each component we have an homogeneous Dirichlet or Neumann boundary condition.

3. MFS and KKM.

3.1. *The MFS in a multiconnected domain.* For simplicity, we present the results concerning the MFS in a two connected domain. The general case can be handled in the same manner. Recall that $\Omega_c = \Omega \setminus \overline{\omega}$, where $\omega, \Omega \subset \mathbb{R}^d$ ($d = 2, 3$) are open and simply connected.

The complementary set $\mathbb{R}^d \setminus \overline{\Omega_c}$ has two connected components, one exterior $\Omega^{\mathrm{C}} = \mathbb{R}^d \setminus \bar{\Omega}$ and one interior, ω.

To apply the Method of Fundamental Solutions, we will consider artificial sets that will define the location of the point-sources. In ω, we consider as admissible sets, $\widehat{\gamma} = \partial\widehat{\omega}$ internal regular boundary of $\widehat{\omega}$ simply connected open set such that $\overline{\widehat{\omega}} \subset \omega$. Finally, we define an external boundary $\widehat{\Gamma} = \partial\widehat{\Omega}$ with $\widehat{\Omega}$ an open unbounded set $\overline{\widehat{\Omega}} \subset \Omega^{\mathrm{C}}$ with a boundary that encloses the domain Ω.

Recall that the fundamental solution for the Lamé system is given by the tensor

$$[\Phi(\mathbf{x})]_{ij} = \begin{cases} \frac{\lambda+3\mu}{4\pi\mu(\lambda+2\mu)} \left[-\log|\mathbf{x}|\delta_{ij} + \frac{\lambda+\mu}{\lambda+3\mu}\frac{x_i x_j}{|\mathbf{x}|^2}\right] & \text{2D case} \\ \frac{\lambda+3\mu}{8\pi\mu(\lambda+2\mu)} \left[\frac{1}{|\mathbf{x}|}\delta_{ij} + \frac{\lambda+\mu}{\lambda+3\mu}\frac{x_i x_j}{|\mathbf{x}|^3}\right] & \text{3D case} \end{cases}$$

and define the source tensor $\Phi_y(x) := \Phi(x-y)$.

Consider the single and double layer potential given in the integral form on a boundary S,

$$\mathbf{L}_S(\phi)(x) = \int_S \Phi_x(y)\phi(y)dS_y, \qquad x \in \mathbb{R}^d \setminus S$$

$$\mathbf{M}_S\psi(x) = \int_S \partial^*_{\lambda,\mu}\Phi_x(y)\psi(y)dS_y, \qquad x \in \mathbb{R}^d \setminus S$$

with $\phi \in H^{-1/2}(S)^d, \psi \in H^{1/2}(S)^d$. The derivative of the tensor Φ_y appearing on the double layer potential is defined as the tensor $[\partial^*_{\lambda,\mu}(\Phi_y\mathbf{e}_i)]_i$ where $(\mathbf{e}_1, \ldots, \mathbf{e}_d)$ is the standard basis of $\mathbb{R}^d$.

Define the operator

$$\mathcal{M}(\Gamma,\gamma) : H^{-1/2}(\widehat{\Gamma})^d \times H^{-1/2}(\widehat{\gamma})^d \longrightarrow H^{1/2}(\Gamma)^d \times H^{(-1)^a 1/2}(\gamma)^d$$

by

$$\mathcal{M}(\Gamma,\gamma)(\phi,\psi) = \begin{bmatrix} \tau_\Gamma \mathbf{L}_{\widehat{\Gamma}} & \tau_\Gamma \mathbf{L}_{\widehat{\gamma}} \\ \mathcal{B}_\gamma \mathbf{L}_{\widehat{\Gamma}} & \mathcal{B}_\gamma \mathbf{L}_{\widehat{\gamma}} \end{bmatrix} \begin{bmatrix} \phi \\ \psi \end{bmatrix}$$

where τ_S is the trace, $\tau_S^{\mathbf{n}} = \partial^*_{\lambda,\mu}$ the normal trace and

$$\mathcal{B}_S = a\tau_S^{\mathbf{n}} + \mathbf{Z}_a\tau_S$$

as in (2).

We show that in the 2D case, $\mathcal{M}(\Gamma,\gamma)$ is injective in $\mathcal{H}_{\mathbf{I}}^{-1/2}(\widehat{\Gamma}\cup\widehat{\gamma})^2$ and has dense range in $\mathcal{H}_{\mathbf{I}}^{1/2}(\Gamma)^2 \times \mathcal{H}_{\mathbf{Z}_a}^{(-1)^a 1/2}(\gamma)^2$, where

$$\mathcal{H}_{\mathbf{R}}^{r}(S)^2 = \left\{\psi \in H^r(S)^2 : \int_S \mathbf{R}(x)\psi(x)dS_x = \mathbf{0}\right\}.$$

Note that if $\int_S \mathbf{R}(x)dS_x$ is invertible then the map $\psi \mapsto \psi + \mathbf{C}$ defines an isomorphism between $\mathcal{H}_{\mathbf{R}}^{r}(S)^2$ and $H^r(S)^2/\mathbb{R}^2$.

Theorem 5. *$\mathcal{M}(\Gamma,\gamma)$ is injective in $\mathcal{H}_{\mathbf{I}}^{-1/2}(\widehat{\Gamma}\cup\widehat{\gamma})^2$.*

Proof. Let $\phi \in \mathcal{H}_{\mathbf{I}}^{-1/2}(\widehat{\Gamma}\cup\widehat{\gamma})^2$ be such that $\mathcal{M}(\Gamma,\gamma)(\phi\Big|_{\widehat{\Gamma}}, \phi\Big|_{\widehat{\gamma}}) = \mathbf{0}$. Denote by $\mathbf{u}$ the single layer potential on $\widehat{\Gamma}\cup\widehat{\gamma}$ with density ϕ, ie.,

$$\mathbf{u} = \mathbf{L}_{\widehat{\Gamma}\cup\widehat{\gamma}}\phi = \mathbf{L}_{\widehat{\Gamma}}\phi\Big|_{\widehat{\Gamma}} + \mathbf{L}_{\widehat{\gamma}}\phi\Big|_{\widehat{\gamma}}.$$

Then,

$$\begin{cases} \Delta^*_{\lambda,\mu}\mathbf{u} = \mathbf{0} & \text{in } \mathbb{R}^2 \setminus (\widehat{\Gamma}\cup\widehat{\gamma}) \\ \mathbf{u} = \mathbf{0} & \text{on } \Gamma \\ \mathcal{B}_\gamma \mathbf{u} = \mathbf{0} & \text{on } \gamma \end{cases} \tag{6}$$

• Since problem (6) restricted to Ω_c is well posed in $H^1(\Omega_c)^2$ we have $\mathbf{u} = \mathbf{0}$ in Ω_c and, by analytic continuation, $\mathbf{u} = \mathbf{0}$ in $\widehat{\Omega}_c$, where $\widehat{\Omega}_c$ is the open and connected domain such that $\partial\widehat{\Omega}_c = \widehat{\Gamma}\cup\widehat{\gamma}$. In particular, $\mathbf{u}^-|_{\widehat{\Gamma}\cup\widehat{\gamma}} = \mathbf{0}$ and $\partial^*_{\lambda,\mu}\mathbf{u}^-|_{\widehat{\Gamma}\cup\widehat{\gamma}} = \mathbf{0}$. Since $\mathbf{u}$ is continuous across $\widehat{\Gamma}\cup\widehat{\gamma}$, we must have $\mathbf{u}^+|_{\widehat{\Gamma}\cup\widehat{\gamma}} = \mathbf{0}$.

• Regarding the unbounded component $\widehat{\Omega}$ we consider the well posed problem (cf. [**11**])

$$\begin{cases} \Delta^*_{\lambda,\mu}\mathbf{u} = \mathbf{0} & \text{in } \widehat{\Omega} \\ \mathbf{u} = \mathbf{0} & \text{on } \widehat{\Gamma} = \partial\widehat{\Omega} \\ \mathbf{u}(x) = \log|x|\ \mathbf{c} + \mathcal{O}(1) & |x| \to \infty \end{cases} \tag{7}$$

with

$$\mathbf{c} = -\frac{\lambda + 3\mu}{4\pi\mu(\lambda+2\mu)}\int_{\widehat{\Gamma}\cup\widehat{\gamma}} \phi(y)dS_y.$$

Now $\mathbf{u}^+$ satisfies this exterior problem with $\mathbf{c} = \mathbf{0}$ therefore, $\mathbf{u}^+ = \mathbf{0}$ in $\widehat{\Omega}$. This implies $\mathbf{u}^+|_{\widehat{\Gamma}} = \mathbf{0}$ and $\partial^*_{\lambda,\mu}\mathbf{u}^+|_{\widehat{\Gamma}} = \mathbf{0}$.

- For the exterior and bounded component $\widehat{\omega}$, the well posed problem

$$\begin{cases} \Delta^*_{\lambda,\mu}\mathbf{u} = \mathbf{0} & \text{in } \widehat{\omega} \\ \mathbf{u} = \mathbf{0} & \text{on } \widehat{\gamma} = \partial\widehat{\omega} \end{cases}$$

is satisfied by $\mathbf{u}^+$. This gives $\mathbf{u}^+ = 0$ in $\widehat{\omega}$ and we conclude that $\mathbf{u}^+|_{\widehat{\gamma}} = \mathbf{0}$ and $\partial^*_{\lambda,\mu}\mathbf{u}^+|_{\widehat{\gamma}} = \mathbf{0}$.

Since ϕ is the boundary jump $[\partial^*_{\lambda,\mu}\mathbf{u}]_{\widehat{\Gamma}\cup\widehat{\gamma}}$ then, from the previous points, we conclude that $\phi = \mathbf{0}$. □

Lemma 6. *The adjoint of $\mathcal{M}(\Gamma,\gamma)$ is*

$$\mathcal{M}(\Gamma,\gamma)^* = \begin{bmatrix} \tau_{\widehat{\Gamma}}\mathbf{L}_\Gamma & \tau_{\widehat{\Gamma}}(a\mathbf{M}_\gamma + \mathbf{L}_\gamma\mathbf{Z}_a) \\ \tau_{\widehat{\gamma}}\mathbf{L}_\Gamma & \tau_{\widehat{\gamma}}(a\mathbf{M}_\gamma + \mathbf{L}_\gamma\mathbf{Z}_a) \end{bmatrix}$$

Proof. We have

$$\begin{aligned} \left\langle \mathcal{B}_\gamma \mathbf{L}_{\widehat{\Gamma}}\phi, \psi \right\rangle_\gamma &= \int_\gamma (a\partial^*_{\lambda,\mu} + \mathbf{Z}_a(x)) \int_{\widehat{\Gamma}} \Phi_x(y)\phi(y)dS_y\psi(x)dS_x \\ &= \int_{\widehat{\Gamma}}\int_\gamma (a\partial^*_{\lambda,\mu} + \mathbf{Z}_a(x))\Phi_y(x)\psi(x)dS_x\phi(y)dS_y \\ &= \left\langle \tau_{\widehat{\Gamma}}\left((a\mathbf{M}_\gamma + \mathbf{L}_\gamma\mathbf{Z}_a)\psi\right), \phi \right\rangle_{\widehat{\Gamma}} \end{aligned}$$

therefore $(\mathcal{B}_\gamma\mathbf{L}_{\widehat{\Gamma}})^* = \tau_{\widehat{\Gamma}}(a\mathbf{M}_\gamma + \mathbf{L}_\gamma\mathbf{Z}_a)$. The other cases can be proved using the same argument. □

Theorem 7. *The operator $\mathcal{M}(\Gamma,\gamma)$ has dense range in $\mathcal{H}^{1/2}_{\mathbf{I}}(\Gamma)^2 \times \mathcal{H}^{(-1)^a 1/2}_{\mathbf{Z}_a}(\gamma)^2$.*

Proof. To prove the density of the range we show that the adjoint $\mathcal{M}(\Gamma,\gamma)^*$ is injective. Let $(\phi,\psi) \in \mathcal{H}^{1/2}_{\mathbf{I}}(\Gamma)^2 \times \mathcal{H}^{(-1)^a 1/2}_{\mathbf{Z}_a}(\gamma)^2$ such that $\mathcal{M}(\Gamma,\gamma)^*(\phi,\psi) = \mathbf{0}$. Define the boundary layer

$$\mathbf{u} = \mathbf{L}_\Gamma\phi + (a\mathbf{M}_\gamma + \mathbf{L}_\gamma\mathbf{Z}_a)\psi.$$

It is clear that

$$(9)\quad [\mathbf{u}]_\Gamma = \mathbf{0}, \quad [\partial^*_{\lambda,\mu}\mathbf{u}]_\Gamma = \phi, \quad [\mathbf{u}]_\gamma = -a\psi \quad \wedge \quad [\partial^*_{\lambda,\mu}\mathbf{u}]_\gamma = \mathbf{Z}_a\psi.$$

We follow the proof of Theorem 5.

• First note that the well posed exterior problem (7) (with $\mathbf{c} = -\frac{\lambda+3\mu}{4\pi\mu(\lambda+2\mu)}(\int_\Gamma \phi(y)dS_y + \int_\gamma \mathbf{Z}_a\psi(y)dS_y))$ is satisfied by $\mathbf{u}^+$ with $\mathbf{c} = \mathbf{0}$. By analytic continuation, it follows that $\mathbf{u}^+ = \mathbf{0}$ in Ω^{C} hence, $\mathbf{u}^+|_\Gamma = \mathbf{0}$ and $\partial^*_{\lambda,\mu}\mathbf{u}^+|_\Gamma = \mathbf{0}$.

• From $\Delta^*_{\lambda,\mu}\mathbf{u}^+ = \mathbf{0}$ in $\widehat{\omega}$ and $\mathbf{u}^+ = \mathbf{0}$ on $\widehat{\gamma} = \partial\widehat{\omega}$ we conclude that $\mathbf{u}^+|_\gamma = \mathbf{0}$ and $\partial^*_{\lambda,\mu}\mathbf{u}^+|_\gamma = \mathbf{0}$.

• Using the jump relations (9), $\mathbf{u}^-$ satisfies the well posed problem

$$(10)\qquad \begin{cases} \Delta^*_{\lambda,\mu}\mathbf{u} = \mathbf{0} & \text{in } \Omega_c \\ \mathbf{u} = \mathbf{0} & \text{on } \Gamma \\ \mathcal{B}_\gamma\mathbf{u} = \mathbf{0} & \text{on } \gamma \end{cases}$$

hence, $\mathbf{u}^-|_\Gamma = \mathbf{u}^-|_\gamma = \mathbf{0}$ and $\partial^*_{\lambda,\mu}\mathbf{u}^-|_\Gamma = \partial^*_{\lambda,\mu}\mathbf{u}^-|_\gamma = \mathbf{0}$.

Thus $\phi = \mathbf{0}$, $a\psi = \mathbf{0}$ and $\mathbf{Z}_a\psi = \mathbf{0}$ and it follows (recall that $a \in \{0, 1\}$ is constant and $\mathbf{Z}_0 = \mathbf{I}$)

$$\phi = \psi = \mathbf{0}. \qquad \square$$

Remark 8.

1. The spaces $\mathcal{H}^r_{\mathbf{Z}}$ are only needed to control the asymptotic behavior of $\mathbf{u}$ at infinity. In fact, taking for instance $\widehat{\Omega}$ bounded, there is no need to add the constants. Although theoretically simpler, this approach (when $\widehat{\Gamma}$ does not enclose the domain Ω) gives worst numerical results.

2. In the 3D case, the asymptotic behavior for the exterior problem is $\mathcal{O}(|x|^{-1})$, which is automatically satisfied by the fundamental solution. In this case, $\mathcal{M}(\Gamma, \gamma)$ is injective in $H^{-1/2}(\widehat{\Gamma} \cup \widehat{\gamma})^3$ with dense range in $H^{1/2}(\Gamma)^3 \times H^{-1/2}(\gamma)^3$, regardless $\widehat{\Omega}$ is unbounded or not.

We now address the question of solving the direct problem (1) with the MFS approximation given by the system

$$(11)\qquad \begin{bmatrix} \tau_\Gamma\mathbf{L}_{\widehat{\Gamma}} & \tau_\Gamma\mathbf{L}_{\widehat{\gamma}} \\ \mathcal{B}_\gamma\mathbf{L}_{\widehat{\Gamma}} & \mathcal{B}_\gamma\mathbf{L}_{\widehat{\gamma}} \end{bmatrix} \begin{bmatrix} \phi \\ \psi \end{bmatrix} = \begin{bmatrix} \mathbf{g} \\ \mathbf{0} \end{bmatrix}.$$

By Theorem 5, the set $\left\{(\Phi_y|_\Gamma, \mathcal{B}_\gamma \Phi_y) : y \in \widehat{\Gamma} \cup \widehat{\gamma}\right\}$ is linearly independent, hence a basis of the space (for simplicity, we suppress the constant functions)

$$\mathcal{S} = \operatorname{span}\left\{(\Phi_y|_\Gamma, \mathcal{B}_\gamma \Phi_y) : y \in \widehat{\Gamma} \cup \widehat{\gamma}\right\}. \tag{12}$$

On the other hand, the density proved in Theorem 7 shows that the pair of input data for problem (1) can be approximated in $\mathcal{S}$. Thus, we consider as approximation for the solution of (1)

$$\widetilde{u} = \sum_{j=1}^{m} \alpha_j \Phi_{y_j} \tag{13}$$

and compute the vectorial coefficients $\alpha_j = (\alpha_{j,1}, \alpha_{j,2})$ such that

$$\sum_{j=1}^{m} \alpha_j \left(\Phi_{y_j}(x_i^\Gamma), \mathcal{B}_\gamma \Phi_{y_j}(x_i^\gamma)\right) = (\mathbf{g}(x_i^\Gamma), \mathbf{0}),$$

on some collocation points $x_1^\Gamma, \ldots, x_{n_1}^\Gamma \in \Gamma$, $x_1^\gamma, \ldots, x_{n_2}^\gamma \in \gamma$ and source points $y_1, \ldots, y_m \in \widehat{\Gamma} \cup \widehat{\gamma}$. When $n_1 + n_2 =: n = m$ this can be done by solving the linear system

$$\mathbf{M}(\Gamma, \gamma)\mathbf{X} = \mathbf{B} \tag{14}$$

with

$$\mathbf{M}(\Gamma, \gamma) = \begin{bmatrix} \Phi_{y_1}(x_1^\Gamma) & \ldots & \Phi_{y_m}(x_1^\Gamma) \\ \ldots & \ldots & \ldots \\ \Phi_{y_m}(x_{n_1}^\Gamma) & \ldots & \Phi_{y_m}(x_{n_1}^\Gamma) \\ \mathcal{B}_\gamma \Phi_{y_1}(x_1^\gamma) & \ldots & \mathcal{B}_\gamma \Phi_{y_m}(x_1^\gamma) \\ \ldots & \ldots & \ldots \\ \mathcal{B}_\gamma \Phi_{y_1}(x_{n_2}^\gamma) & \ldots & \mathcal{B}_\gamma \Phi_{y_m}(x_{n_2}^\gamma) \end{bmatrix},$$

$$\mathbf{X} = \begin{bmatrix} \alpha_1 \\ \vdots \\ \alpha_n \end{bmatrix}, \ \mathbf{B} = \begin{bmatrix} \mathbf{g}(x_1) \\ \vdots \\ \mathbf{g}(x_{n_1}) \\ \mathbf{0} \\ \vdots \\ \mathbf{0} \end{bmatrix},$$

and for overdetermined systems ($n > m$) in a least squares sense, ie., solving the system

$$\mathbf{M}(\Gamma,\gamma)^\top \mathbf{M}(\Gamma,\gamma)\mathbf{X} = \mathbf{M}(\Gamma,\gamma)^\top \mathbf{B}.$$

3.2. *MFS version of the KKM.* We now consider the inverse problem, ie., to obtain the shape of the boundary γ from the Cauchy data on Γ. The Kirsch-Kress Method (cf. [**20**]) was initially presented for acoustic scattering (twenty years ago), and the external boundary Γ was then replaced by the knowledge of the far field pattern.

The method consists in assuming that some knowledge on γ exists, such that we can prescribe an artificial boundary $\widehat{\gamma}$ inside γ and write the solution in terms of the inner boundary layer representation.

In the acoustic scattering problem the unknown density for the artificial inner boundary layer was recovered fitting its far field pattern. In the bounded domain we need to fit the Cauchy data and it is clear that the inner boundary will not be enough to adjust both Dirichlet and Neumann data. An extra external boundary layer must be considered.

At least two adaptations could be possible for the bounded domain:

(a) Use the boundary element method (BEM) formulation, and the extra boundary layer would be defined on the external accessible boundary Γ.

(b) Use the method of fundamental solutions (MFS) and define an external artificial boundary layer $\hat{\Gamma}$.

We will consider the second approach, and therefore it should be considered that we will use the MFS adaptation of the Kirsch-Kress Method (KKM).

Therefore the MFS version of the KKM method for the inverse bounded problem consists in two steps:

(i) **linear part:** solving the system of integral equations

$$\underbrace{\begin{bmatrix} \tau_\Gamma \mathbf{L}_{\widehat{\Gamma}} & \tau_\Gamma \mathbf{L}_{\widehat{\Gamma}} \\ \tau_\Gamma^{\mathbf{n}} \mathbf{L}_{\widehat{\Gamma}} & \tau_\Gamma^{\mathbf{n}} \mathbf{L}_{\widehat{\Gamma}} \end{bmatrix}}_{\mathcal{K}(\Gamma,\Gamma)} \begin{bmatrix} \phi|_{\widehat{\Gamma}} \\ \phi|_{\widehat{\Gamma}} \end{bmatrix} = \begin{bmatrix} \mathbf{g} \\ \partial^*_{\lambda,\mu}\mathbf{u} \end{bmatrix}, \tag{15}$$

where τ_Γ, $\tau_\Gamma^{\mathbf{n}}$ are, respectively the trace and the normal trace on Γ. Note that $\mathcal{K}(\Gamma,\Gamma)$ is $\mathcal{M}(\Gamma,\Gamma)$ with $\mathcal{B}_\Gamma = \tau_\Gamma^{\mathbf{n}}$, when $\gamma = \Gamma$.

(ii) **nonlinear part:** the boundary γ will be given by the level set $\mathbf{u}^{-1}(\mathbf{0}) = \{x \in \Omega : \mathbf{u}(x) = \mathbf{0}\}$, for the Dirichlet problem (or computed iteratively, in an optimization scheme for a class of approximating shapes, for the Neumann or other boundary condition).

The linear part of the Kirsch-Kress Method to solve the Cauchy problem is therefore connected to the MFS since it may use the same boundary layers on $\widehat{\gamma}$ and on $\widehat{\Gamma}$ to approximate the solution of the direct problem from the boundary conditions on γ and Γ, and the reconstruction of the solution from the Dirichlet and Neumann data on Γ. In fact, the first line of (15) would be the same – known Dirichlet data.

As in the direct MFS (11), the system of equations (15) may not have a solution, even for exact boundary data.

We will now present density results showing that a pair of Cauchy data can be approximated using the MFS version of the KKM method. Nevertheless, both (11) and (15) are ill posed integral systems, and regularization techniques (for instance, Tikhonov regularization) are a way to address ill conditioning arising from integral equations of the first kind (on this subject, we refer for instance the book by Kress [**21**], chapter 15).

Consider the matrix operator $\mathcal{K}(\Gamma,\Gamma) : H^{-1/2}(\widehat{\Gamma} \cup \widehat{\gamma})^2 \longrightarrow H^{1/2}(\Gamma)^2 \times H^{-1/2}(\Gamma)^2$ defined in (15).

Lemma 9. *The operator $\mathcal{K}(\Gamma,\Gamma)$ is injective in $H^{-1/2}(\widehat{\Gamma} \cup \widehat{\gamma})^2/\mathbb{R}^2$ and its adjoint is given by*

$$\mathcal{K}(\Gamma,\Gamma)^* = \begin{bmatrix} \tau_{\hat{\Gamma}} \mathbf{L}_\Gamma & \tau_{\hat{\Gamma}} \mathbf{M}_\Gamma \\ \tau_{\hat{\gamma}} \mathbf{L}_\Gamma & \tau_{\hat{\gamma}} \mathbf{M}_\Gamma \end{bmatrix}$$

Proof. To show the injectivity, suppose that $\mathcal{K}(\Gamma,\Gamma)(\phi) = \mathbf{0}$. Then, considering the single layer potential $\mathbf{u}(x) = \mathbf{L}_{\widehat{\Gamma}\cup\widehat{\gamma}}(\phi)(x),\ x \in \mathbb{R}^2 \setminus (\widehat{\Gamma} \cup$

$\widehat{\gamma}$) we have

$$\begin{cases} \Delta^*_{\lambda,\mu}\mathbf{u} = \mathbf{0} & \text{in } \mathbb{R}^2 \setminus (\widehat{\Gamma} \cup \widehat{\gamma}) \\ \mathbf{u} = \mathbf{0} & \text{on } \Gamma \\ \partial^*_{\lambda,\mu}\mathbf{u} = \mathbf{0} & \text{on } \Gamma \end{cases}$$

By Lemma 1, $\mathbf{u} = \mathbf{0}$ in the open connected set $\widehat{\Omega}_c$ such that $\partial\widehat{\Omega}_c = \widehat{\Gamma}\cup\widehat{\gamma}$. Thus, the trace $\mathbf{u}^-|_{\widehat{\Gamma}\cup\widehat{\gamma}}$ and normal trace $\partial^*_{\lambda,\mu}\mathbf{u}^-|_{\widehat{\Gamma}\cup\widehat{\gamma}}$ are null. On the other hand, the boundary jumps across $\widehat{\Gamma} \cup \widehat{\gamma}$ are given by

$$[\mathbf{u}]_{\widehat{\Gamma}\cup\widehat{\gamma}} = \mathbf{0} \ \wedge \ [\partial^*_{\lambda,\mu}\mathbf{u}]_{\widehat{\Gamma}\cup\widehat{\gamma}} = \phi$$

and therefore, $\mathbf{u}^+|_{\widehat{\Gamma}\cup\widehat{\gamma}}$ is null. Following the proof of Theorem 5 (now $\mathbf{c} = \frac{\lambda+3\mu}{4\pi\mu(\lambda+2\mu)} \int_{\widehat{\Gamma}\cup\widehat{\gamma}} \phi dS_x = \mathbf{0}$), we conclude that the exterior traces $\partial^*_{\lambda,\mu}\mathbf{u}^+|_{\widehat{\Gamma}\cup\widehat{\gamma}}$ are also null and it follows that $\phi = \mathbf{0}$.

The adjoint can be easily computed, following the proof of Lemma 6. □

Theorem 10. *The matrix operator* $\mathcal{K}(\Gamma,\Gamma)$ *has dense range in* $H^{1/2}(\Gamma)^2/\mathbb{R}^2 \times H^{-1/2}(\Gamma)^2$.

Proof. Again, we follow the proof of Theorem 5. We identify the space $\mathcal{H}^{1/2}_{\mathbf{I}}(\Gamma)^2$ with $H^{1/2}(\Gamma)^2/\mathbb{R}^2$. Let $\psi \in \mathcal{H}^{1/2}_{\mathbf{I}}(\Gamma)^2, \phi \in H^{-1/2}(\Gamma)^2$ and define the function

$$\mathbf{u}(y) = (\mathbf{L}_\Gamma\psi)(y) + (\mathbf{M}_\Gamma\phi)(y)$$

a combination of single and double layer potentials defined on Γ. Now, if $\tau_{\widehat{\Gamma}\cup\widehat{\gamma}}\mathbf{u} = \mathcal{K}(\Gamma,\Gamma)(\psi,\phi)= \mathbf{0}$ then by analytic continuation of the unique null solution of the interior and exterior problems ($\mathbf{c} = \frac{\lambda+3\mu}{4\pi\mu(\lambda+2\mu)} \int_\Gamma \psi(x) dS_x = \mathbf{0}$,), we obtain $\mathbf{u} = \mathbf{0}$ in $\mathbb{R}^2 \setminus \Gamma$. Then $\psi = [\partial^*_{\lambda,\mu}\mathbf{u}]_\Gamma= \mathbf{0}$, $\phi = -[\mathbf{u}]_\Gamma= \mathbf{0}$ and the result follows. □

Remark 11. If $\widehat{\Omega}$ is bounded, the injectivity can be established in $H^{-1/2}(\widehat{\Gamma} \cup \widehat{\gamma})^2$ and the density of the range in $H^{1/2}(\Gamma)^2 \times H^{-1/2}(\Gamma)^2$. Again, for the 3D case, there is no need to add the constants.

This suggests the use of (13) to approximate the solution of the system (15). Now, the vectorial coefficients must be computed in order to obtain

$$\sum_{j=1}^{m} \alpha_j (\Phi_{y_j}, \partial^*_{\lambda,\mu}\Phi_{y_j})|_\Gamma = (\mathbf{g}, \partial^*_{\lambda,\mu}\mathbf{u}) \tag{16}$$

for some source points $y_1, \dots, y_m \in \widehat{\Gamma} \cup \widehat{\gamma}$. As usual, we proceed by imposing (16) on some collocation points $x_1, \dots, x_n \in \Gamma$, thus obtaining a discrete version of (15) for $n = m$ and a least squares version, if $n > m$. In general the measured data is affected by noise hence, some regularization scheme must be considered.

Remark 12. The density results prove that an approximation is possible, however since the proof is not constructive we do not have an algorithm that gives us the appropriate choices for source and collocation points in MFS based methods. For Laplace equation, exponential convergence of the MFS, for smooth data and appropriate chosen source points, has been proven for circles or its conformal mapped domains (eg. [**7, 17, 18, 25**]). On the other hand, this optimal exponential decay of the error $O(R^{-n})$ has a counterpart of exponential increase of the condition number $O(R^n)$, for a circle of radius R (cf. [**19**]). This leads to an "uncertainty principle" already pointed out for RBF approximations (cf. [**29**]): we can not get both accurate approximations and low condition numbers. In the next section, we present numerical simulations for the MFS (direct problem) and the MFS–KKM (inverse problem). In Table 1 we present maximum errors and computed condition numbers for the MFS, for a non trivial shape. We may notice that despite early high condition numbers, the MFS presents increasing accurate approximations. Under regularity assumptions, still one limitation to MFS performance concerns machine precision. Unlike other classical methods, the MFS presents accurate results much sooner, and ill conditioning problems also appear in an early stage. The ill conditioning limitation can be circumvented using regularization techniques (with some loss in accuracy) or higher machine precision calculations (with some loss in computation time).

Remark 13. For general domain shapes Ω_c we can perform an optimization scheme to choose the location of the points (eg. [**25**]), but this approach is computational expensive, and when applied to the MFS-KKM requires some *a priori* knowledge of ω. For other approaches to inverse geometric problems in acoustic scattering, we refer the book of Colton and Kress [**12**], where the computation of the density of the single layer potential and γ is made by optimization; or the paper by Potthast and Schulz [**28**], for an adaptation using the range test method. We note that such type of non linear optimization on the shape of ω can be applied to the elastic problem, as it has been made for the Stokes system (cf. [**24**]).

4. Numerical Simulations. In this section we consider three numerical simulations of the MFS - Kirsch-Kress Method applied to the recovery of a single inclusion. The accessible part of the boundary, Γ, is a centered circle with radius $r = 3.5$ and the boundary of the inclusion is given by the parametrization

$$\gamma_i(t) = \mathbf{c}_i + j_i(t)(\cos t, \sin t), \qquad 0 \le t \le 2\pi$$

with $\mathbf{c}_1 = (-1, 1)$, $j_1(t) = 1.1 + 1.6\cos^2(t/2)\sin(t/2)$, $\mathbf{c}_2 = (1, -0.3)$, $j_2(t) = 1.2 + 0.2\cos^2(2t)$, $\mathbf{c}_3 = (0, 0)$ and $j_3(t) = 1.3 - 0.3\cos(4t)$ (see Fig. 1). The Lamé constants are $\lambda = \mu = 1$ and as input function we use

$$\mathbf{g}_i(\mathbf{x}) = \mathbf{x} - \mathbf{c}_i - \nabla \log(|\mathbf{x} - \mathbf{c}_i|)$$

(in particular, we are assuming that the center of the inclusion is known in the inverse problem).

• As mentioned before, the convergence of the method for the direct problem strongly depends on the number and location of source and collocations points. We considered, as artificial boundary,

$$\widehat{\gamma}_i = \partial B(0, 4.2) \cup \gamma_i^{\#},$$

with $\gamma_i^{\#}(t) = \mathbf{c}_i + 0.9 j_i(t)(\cos t, \sin t)$. For this choice of artificial boundary we present in Table 1 the evolution of the condition number of $\mathbf{M}(\Gamma, \gamma)$ and the absolute error on the boundary in terms of the number of (uniformly distributed) source and collocation points, n. This table concerns the first simulation and the error (middle column) was computed taking the maximum norm of the error vector, whose entries are given by pointwise evaluation of the boundary error at 600 (non collocation) boundary points. To solve the direct problem for each example, we used 400 collocation and source points (distributed uniformly). In Fig. 2 we plot the absolute error of the first component on Γ and the second component on γ_3.

• For the inverse problem, we used $\partial B(0, 4.0) \cup \partial B(c_i, 0.7)$ as artificial boundary and solved the system of linear equations arising from the discretization of (15) in a least squares sense, using 300 source and 300 collocation points. This avoids the so called *inverse crimes* since the artificial boundaries used in the direct problem are different in the inverse problem as well as the number of collocation points. To retrieve the curve, we performed a search along the segment joining radial points on Γ and on the internal artificial boundary and choose the point with image near zero (in norm). Repeating this procedure for several points on Γ we obtain the approximation of γ.

For exact data, we retrieved the correct shape of the inclusion (first and second simulations). We present the numerical simulations for measured data affected by random (maximum norm) noise, i.e. the input vector is

$$[\partial^*_{\lambda,\mu}\mathbf{u}]_k^{noise} = [\partial^*_{\lambda,\mu}\mathbf{u}]_k + \varepsilon_k ||\partial^*_{\lambda,\mu}\mathbf{u}||_\infty$$

with random values ε_k such that $|\varepsilon_k| \leq \rho < 1$. A Tikhonov regularization procedure was implemented to solve the systems with an L-curve analysis to choose the regularization parameter. Figs. 3 and 4 shows the comparison between the given (noiseless) Cauchy data on Γ and the computed data on the inverse problem (introducing 8 % of random noise in the measured data) for simulations 1 and 2, respectively.

For the first simulation, we present in Fig. 5 the results of the reconstructions with 3% and 8% of random noise.

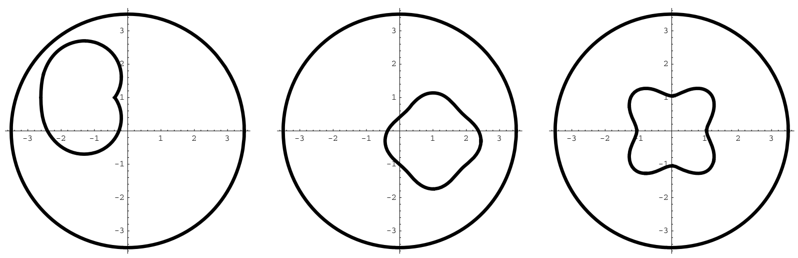

Figure 1. Geometry of the domains. Left- first test, middle- second test and right- third test.

n	Absolute error on the boundary	$\kappa(\mathbf{M}(\Gamma,\gamma))$
50	2.4×10^{-2}	4.2×10^{22}
100	2.2×10^{-3}	1.8×10^{31}
200	4.7×10^{-4}	5.6×10^{25}
300	2.1×10^{-6}	1.3×10^{21}
400	4.5×10^{-7}	3.1×10^{20}
500	4.5×10^{-7}	5.1×10^{20}
600	6.5×10^{-8}	7.2×10^{20}
1000	9.3×10^{-9}	2.4×10^{22}

Table 1. Evolution of the absolute error on the boundary (using the maximum norm) and the condition number of $\mathbf{M}(\Gamma,\gamma)$ with the number of source points n

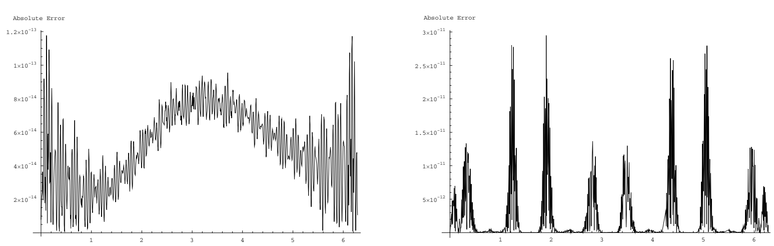

Figure 2. Absolute error on the boundary (third simulation): On the left–first coordinate on Γ, on the right– second coordinate on γ.

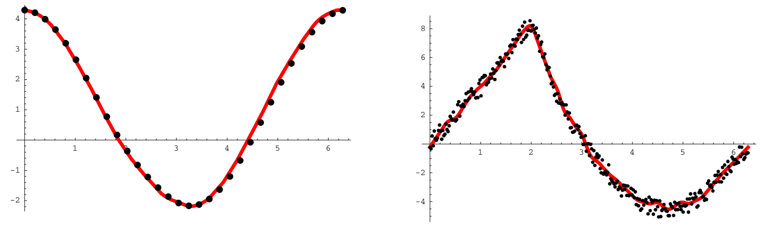

Figure 3. Comparison between the noisy Cauchy data on Γ and the computed data on the inverse problem (first simulation). On the left– first coordinate of the solution, on the right– second coordinate of the traction vector. Dots– data from the direct problem, thick red line– inverse problem. Noise level: 8 %.

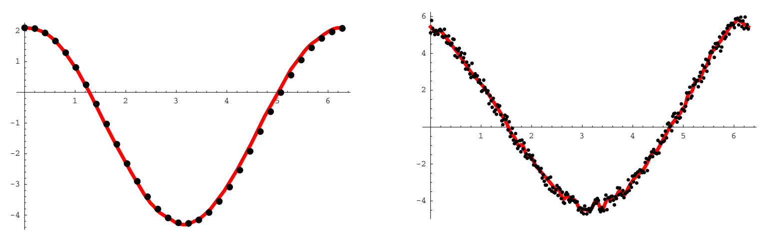

Figure 4. The same as in Fig. 4, for the second simulation. On the right picture we considered the first coordinate of the traction vector.

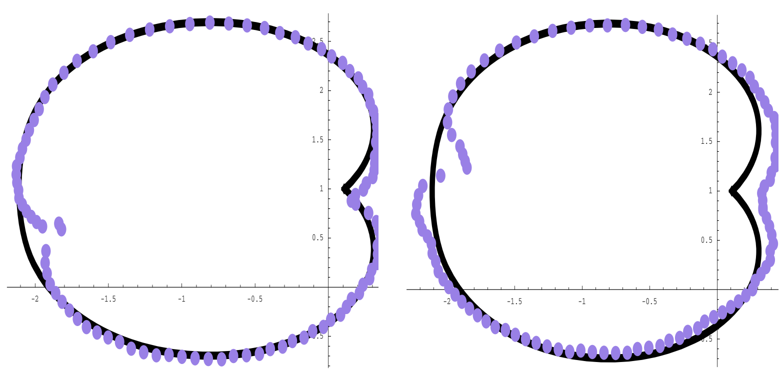

Figure 5. Reconstruction of the shape with 3 % (left) and 8 % (right) of noise. Full line- Shape of the inclusion; Dotted line- Reconstructed curve.

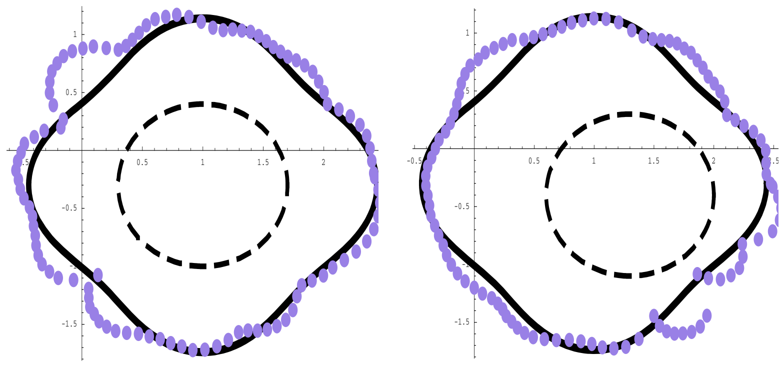

Figure 6. Reconstruction of the shape with internal circle (dashed line) centered with the inclusion (left) and on $(1.3, -0.4)$ (right). Noise level: 8 % .

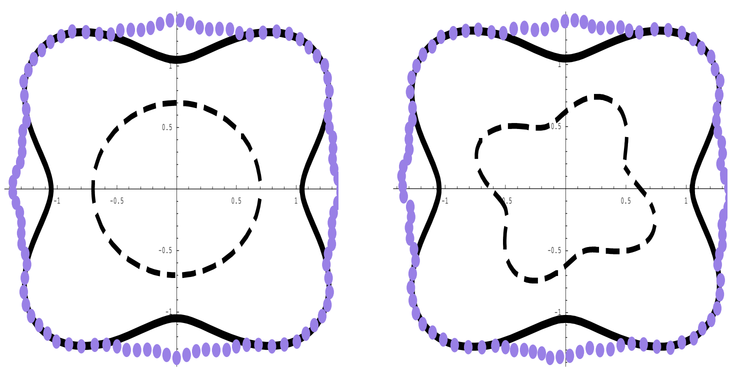

Figure 7. Reconstruction using different internal curves (exact data).

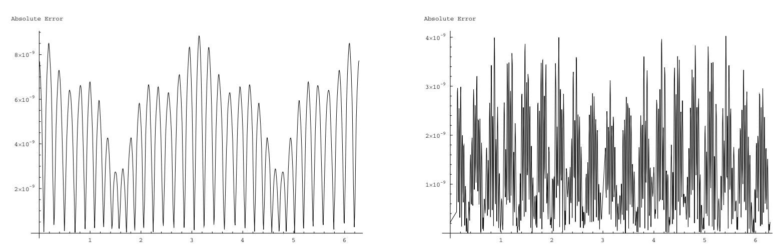

Figure 8. Error on Γ for the computed solution of the Cauchy problem: left- first coordinate; right- second coordinate of the traction vector.

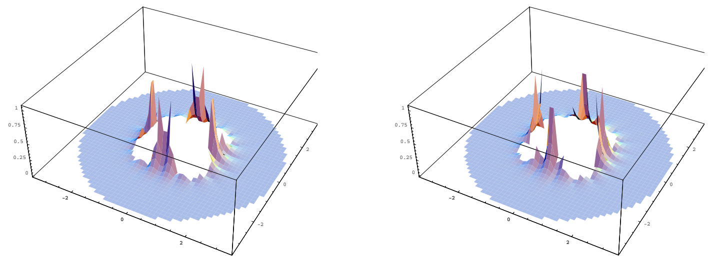

Figure 9. Absolute difference between the solution of the direct problem and the inverse problem: Left- first coordinate; Right- second coordinate.

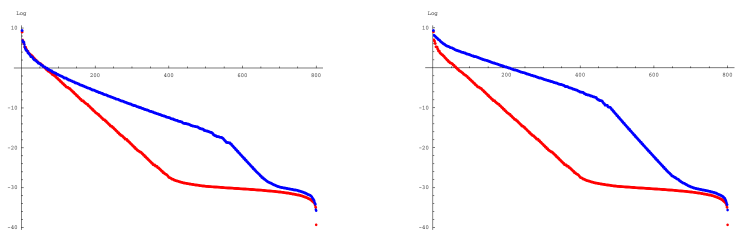

Figure 10. Eigenvalues of the system arising from the discretization of the problems: Left- Inclusion reconstruction (homogeneous Dirichlet condition on γ); Right- cavity reconstruction (homogeneous Neumann condition on γ). Blue (top) curve- direct problem using MFS; Red (bottom) curve- inverse problem using the Kirsch Kress method.

In the second simulation we present the effect of changing the center of the internal artificial curve in the reconstruction of the shape. Here, we tested for the artificial boundary $\partial B(c_2, 0.7)$ and $\partial B((1.3, -0.4), 0.7)$ (see Fig. 6) with 8 % of noise. The result obtained with the second choice of center is slightly better (and the corresponding system of equations is better conditioned) than the centered case.

The third simulation is presented using exact data. For this geometry the results are not so good even when tested with a non convex artificial internal domain (Fig. 7), yet the Cauchy data on Γ is well approximated (Fig. 8). In Fig. 9 we present the absolute difference between the MFS solution of the direct problem and the inverse problem solution, which shows the instabilities that led to the problems observed in the reconstructions. In fact, the distance between the collocation and (inner) source points is bigger in the inverse problem and we observe a faster decay of the inverse problem matrix eigenvalues than in the direct problem (see Fig. 10). Recall that for the direct problem the artificial boundary is close to the boundary of Ω_c leading to a better conditioned system of equations whereas in the inverse problem only the outer part of the boundary is being considered and the internal part of the artificial boundary must be inside the inclusion.

Conclusions. In this work we discussed the question of the identification of inclusions/cavities in an elastic body, using a single boundary measurement. We proved the adequacy of the MFS to solve not only the direct problem, but also to solve the inverse (Cauchy) problem with a MFS version of the Kirsch-Kress Method. We proposed a fast procedure to reconstruct the shape of the inclusion and test it for several examples. In general, we were able to retrieve the localization and dimension of the inclusion and in some cases (mainly convex inclusions) a good reconstruction of the shape, for data affected by random (norm) noise.

Acknowledgments. Authors acknowledge the support of Fundacão para a Ciência e Tecnologia (FCT), through projects POCI MAT/61792/2004, MAT/60863/2004 and ECM/58940/2004. N. Martins is also partially supported by FCT through the scholarship SFRH/BD/27914/2006.

REFERENCES

1. G. Alessandrini, A. Morassi, E. Rosset, *Detecting an inclusion in an elastic body by boundary measurements*, SIAM Review **46**, No. 3, (1994), 477–498.

2. C. J. S. Alves and H. Ammari, *Boundary integral formulae for the reconstruction of imperfections of small diameter in an elastic medium*, SIAM J. Appl. Math, **62**, (2001), 94–106.

3. C. J. S. Alves and C. S. Chen, *A new method of fundamental solutions applied to nonhomogeneous elliptic problems*, Adv. Comp. Math., **23**, (2005), 125–142.

4. H. Ammari, H. Kang, G. Nakamura and K. Kazumi, *Complete asymptotic expansions of solutions of the system of elastostatics in the presence of an inclusion of small diameter and detection of an inclusion*, Journal of Elasticity, **67**(2), (2002), 97–129.

5. E. Argyropoulos and K. Kiriaki, *Modified Green's function technique for disjoint bodies in two-dimensional linear elasticity*, Bull. Greek Math. Soc., **47**, (2003), 137–151.

6. K. Baganas, A. Charalambopoulos and G. D. Manolis, *Detection of spherical inclusions in a bounded, elastic cylindrical domain*, Wave Motion, **41**(1), (2005), 13–28.

7. A. Bogomolny, *Fundamental solutions method for elliptic boundary value problems*, Siam, J. Numer. Anal., **22**, (1985), 644–669.

8. M. Bonnet and A. Constantinescu, *Inverse problems in elasticity*, Inverse Problems, **21**, (2005), R1–R50.

9. K. Bryan and L. Caudill, *An Inverse problem in thermal imaging*, SIAM J. Appl. Math., **56**, (1996), 715–735.

10. F. Cakoni and R. Kress, Integral equations for inverse problems in corrosion detection from partial Cauchy data, Inverse Problems and Imaging, **1**(2), (2007), 229–245.

11. G. Chen and J. Zhou , *Boundary Element Methods*, Academic Press, London, (1992).

12. D. Colton and R. Kress , *Inverse Acoustic and Electromagnetic Scattering Theory*, 2. ed., Applied Mathematical Sciences, 93, Springer, (1998).

13. L. C. Evans, *Partial Differential Equations*, Springer-Verlag, New York, (1991).

14. G. Fairweather and A. Karageorghis, *The method of fundamental solutions for elliptic boundary value problems*, Adv. Comput. Math., **9**, (1998), 69–95.

15. D. Fasino and G. Inglese, *Discrete methods in the study of an inverse problem for Laplace's equation*, IMA Journal of Numerical Analysis, **19**, (1999), 105–118.

16. G. Inglese, *An inverse problem in corrosion detection*, Inverse Problems, **13**, (1997), 977–994.

17. M. Katsurada, *Asymptotic error analysis of the charge simulation method in a Jordan region with an analytic boundary*, J. Fac. Sci. Univ. Tokyo, Sect. IA 37, (1990), 635–657.

18. M. Katsurada and H. Okamoto, *The collocation points of the fundamental solution method for the potential problem*, Computers Math. Applic., **31**(1), (1996), 123–137.

19. T. Kitagawa, *On the numerical stability of the method of fundamental solution applied to the Dirichlet problem.* Japan J. Appl. Math. **5**, (1998), 123–133.

20. A. Kirsch and R. Kress, *On an integral equation of the first kind in inverse acoustic scattering*, Inverse Problems, ISNM **77**, (1986), 93–102.

21. R. Kress, *Linear integral equations*, 2nd Edition, Springer, New York, 1999.

22. V. D. Kupradze and M. A. Aleksidze, *The method of functional equations for the aproximate solution of certain boundary value problems*, Zh. vych. mat., **4**, (1964), 683–715.

23. L. Marin, *A meshless method for solving the Cauchy problem in three-dimensional elastostatics*, Comput. Math. Appl. **50**, (2005), 73-92.

24. N.F.M. Martins and A.L. Silvestre, *An iterative MFS approach for the detection of immersed obstacles*, Eng. Anal. Bound. Elem., **32**(6), (2008), 517-524.

25. R. Mathon and R.L. Johnston, *The approximate solution of elliptic boundary value problems by fundamental solutions*, SIAM J. Numer. Anal. **14**, (1977), 638-650.

26. A. Morassi and E. Rosset, *Detecting rigid inclusions or cavities, in an elastic body*, Journal of elasticity, **73**, (2003), 101–126.

27. G. Nakamura and G. Uhlmann, *Identification of Lamé parameters by boundary measurements*, American Journal of Mathematics, **115**, (1993), 1161–1187.

28. R. Potthast and J. Schulz, *A multi-wave range test for obstacle reconstructions with unknown physical properties*, J. Comput. Appl. Math., **205**(1), (2007), 53–71.

29. R. Schaback, *Error estimates and condition numbers for radial basis function interpolation.* Adv. Comp. Math. **3**, (1995), 251-264.

30. V. S. Vladimirov, *Equations of mathematical physics.* MIR, Moscow, (1984).

CEMAT-IST and Departamento de Matemática, Instituto Superior Técnico (T. U. Lisbon), Av. RoviscoPais 1, 1049-001 LISBOA, PORTUGAL.
Email address: calves@math.ist.utl.pt

CEMAT-IST and Departamento de Matemática, Faculdade de Ciências e Tecnologia, NULisbon, Quinta da Torre, 2829-516 Caparica, Portugal
Email address: nfm@fct.unl.pt